FIGURES

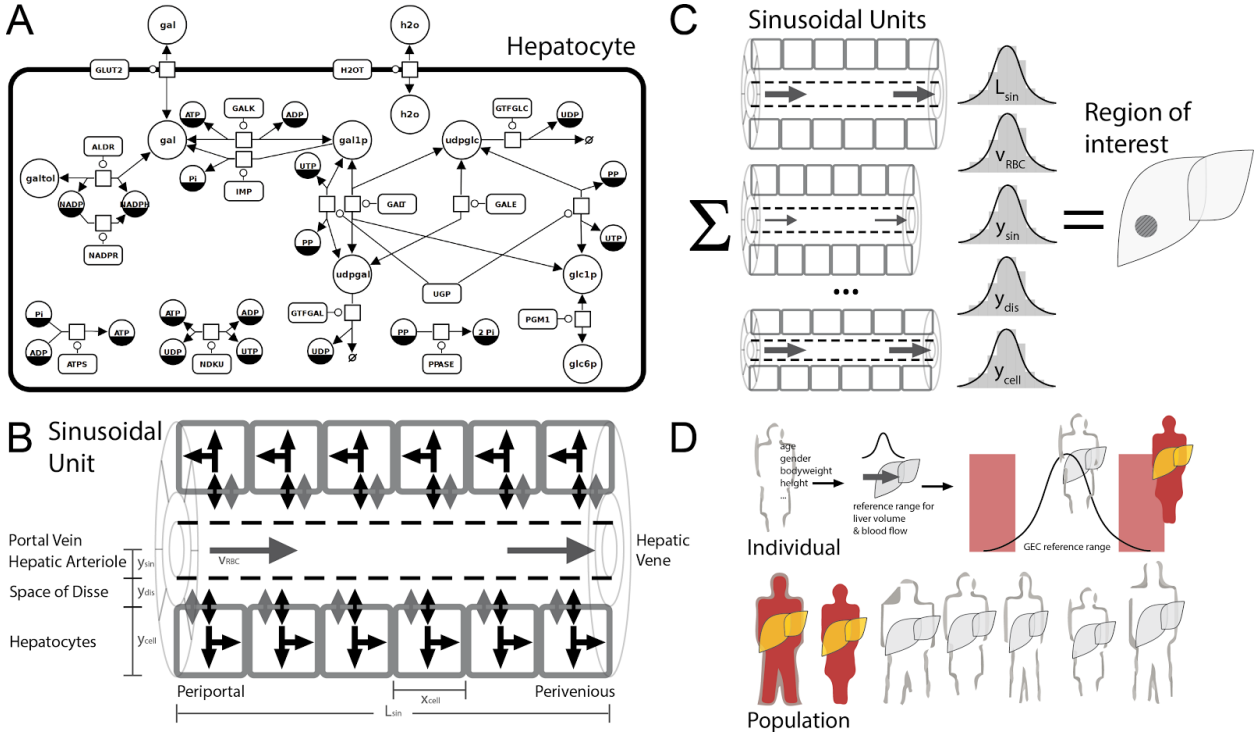

Figure 1 *– Model overview of hepatic galactose metabolism on cellular, tissue- and organ-scale and application in prediction of individual galactose clearance*

A) Overview of detailed kinetic model of hepatic galactose metabolism in SBGN {LeNovere2009}.
Reactions: (ALDR) **Aldose reductase (galactitol NAD 1-oxidoreductase);** (ATPS) **ATP synthesis;** (GALDH) **Galactose 1-dehydrogenase;** (GALE) **UDP-glucose 4-epimerase;** (GALK) **Galactokinase;** (GALT) **Galactose-1-phosphate uridyl transferase;** (GLUT2) **Facilitated glucose transporter member 2;** (GTFGAL) **Glycosyltransferase galactose;** (GTFGLC) **Glycosyltransferase glucose;** (NADPR) **NADP reductase;** (NDKU) **Nucleoside diphosphokinase, ATP:UDP phosphotransferase;** (IMP) **Inositol monophosphatase;** (PGM1) **Phosphoglucomutase-1;** (PPASE) **Pyrophosphatase;** (UGALP) **UDP-galactose pyrophosphorylase;** (UGP) **UDP-glucose pyrophosphorylase;**
Metabolites: (adp) **ADP;** (atp) **ATP;** (gal) **D-galactose;** (gal1p) **D-galactose 1-phosphate;** (galnat) **D-galactonate;** (galtol) **D-galactitol;** (glc) **D-glucose;** (glc1p) **D-glucose 1-phosphate;** (glc6p) **D-glucose 6-phosphate;** (nadp) **NADP;** (nadph) **NADPH;** (pi) **phosphate;** (pp) **pyrophosphate;** (udp) **UDP;** (udpgal) **UDP-D-galactose;** (udpglc) **UDP-D-glucose;** (utp) **UTP;**
B) Tissue-scale model of the sinusoidal unit comprising diffusion and convection based transport of substances in the sinusoid, diffusion-based transport of substances in the space of Disse and description of cellular metabolism via kinetic models of individual hepatocytes. Blood coming from the hepatic artery and portal vein enters the sinusoidal unit periportal and leaves pericentral. Transport between the sinusoid and the space of Disse occurs via fenestrations in the endothelial cells. Parameters and references are provided in the supplement.

C) Region of interests of the liver are modeled via the integration of multiple sinusoidal units based on the observed heterogeneity of structural parameters and microcirculation within the lobulus.
D) Based on anthropomorphic information of subjects like age, gender, bodyweight and height the region of interests are scaled to the observed distributions of liver blood flow and liver volume. Reference values of galactose clearance (GEC) are calculated and the experimental value of GEC can be evaluated in this reference context. Based on available data on the distribution of anthropomorphic features (NHANES {REF}) the population variability can be evaluated.

Figure 2 *– Parameter distributions and resulting multiple-indicator dilution curves*

A

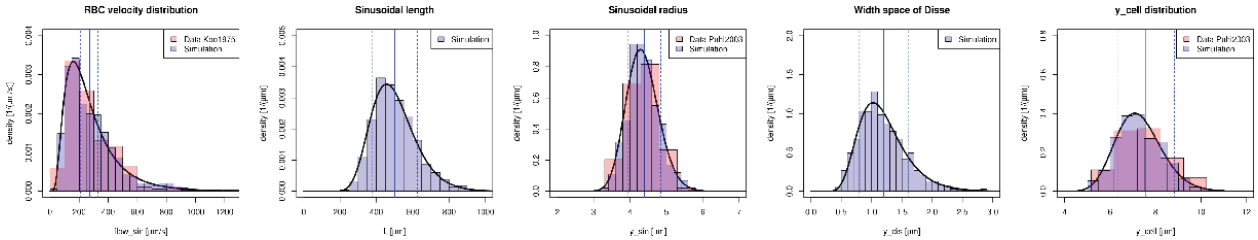

B

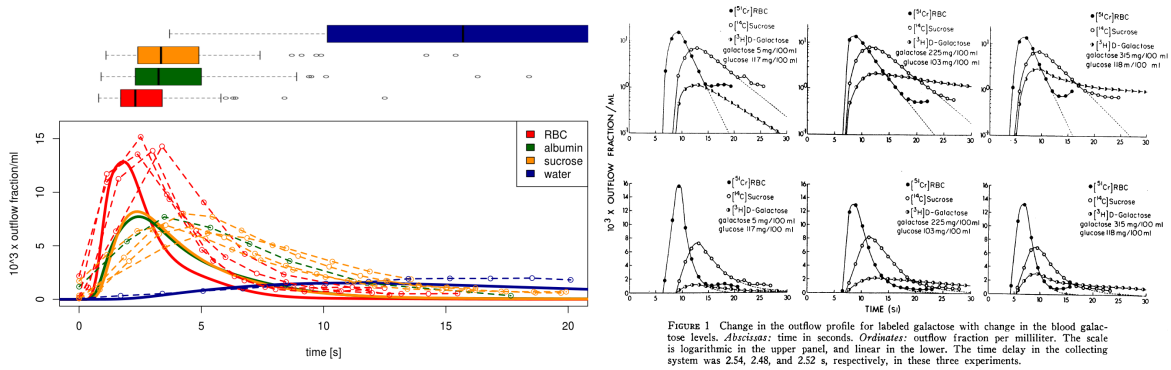

FIGURE 1 Change in the outflow profile for labeled galactose with change in the blood galactose levels. *Abscissas:* time in seconds. *Ordinates:* outflow fraction per milliliter. The scale is logarithmic in the upper panel, and linear in the lower. The time delay in the collecting system was 2.54, 2.48, and 2.52 s, respectively, in these three experiments.

C

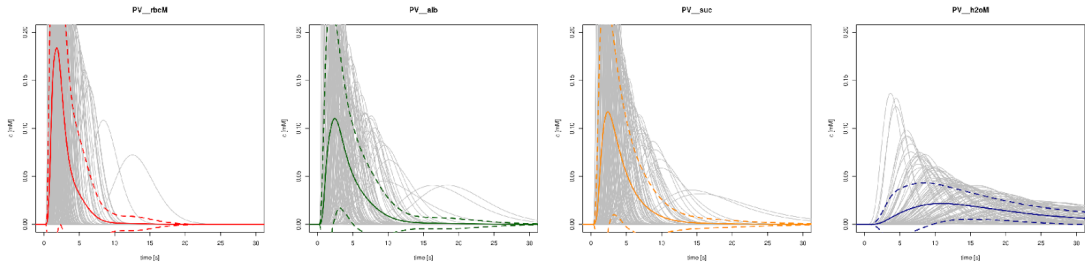

A) Parameter distributions for model simulations. Monte-Carlo simulations are. For every simulation a multitude of structural different sinusoidal units is simulated and the results are integrated. Shown are the parameter distributions based on fitting with the experimental data and the sample for the simulation (N=1000).

B) Predicted multiple-indicator diluation curves based on fixed paramterization of model with literature data. Input peak is rectangle peak with duration of 0.5s. top) Boxplot of simulated peak times of dilution curves for RBC, albumin, sucrose and water. botton) mean Experimental data from dogs dashes (Goresky, et al., 1973) [Goresky1983].

The model reproduces the observed.

C) Individual curves for the sampled geometries with mean (solid) and mean+-std (dashed)

With and without galactose. The response of the different sinusoids is very heterogenous and the actual dilution behavior depends strongly on the local microarchitecture.

Figure 3 *– Hepatic galactose elimination, extraction ratio, and flow-dependent clearance and extraction ratio on tissue scale*

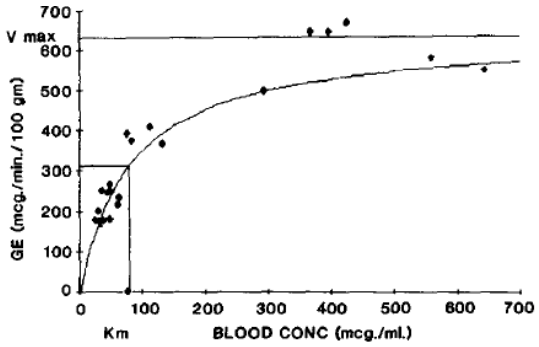

FIG. 1. Galactose elimination kinetics. Points represent individual animals. Superimposed line as determined by the Michaelis–Menten equation using the elimination constants, V_{max} and K_m, from Fig. 2.

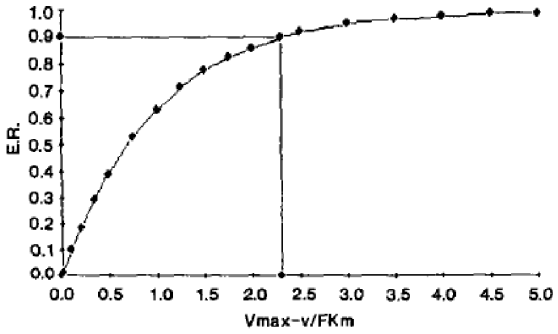

FIG. 4. Extraction ratio as a function of V_{max}/FK_m. Values of $V_{max}/FK_m > 2.3$ are associated with ER > 0.90.

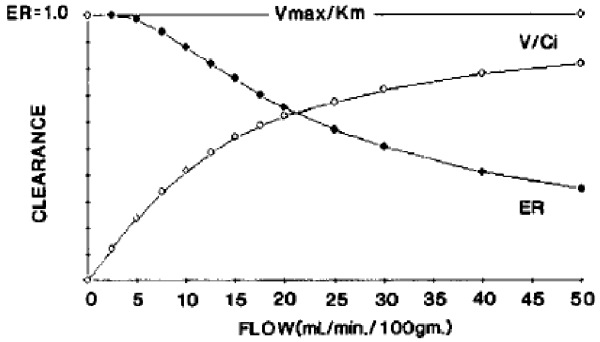

FIG. 6. Clearance and extraction ratio vs flow. Extraction ratio decreases as flow increases. Clearance increases with flow to a maximum of V_{max}/K_m.

(Schirmer, et al., 1986)

GEC clearance curves and extraction ratios

Changes in GEC clearance due to fenestraetion & aging (show the curves with the experimental data).

Figure 4 *– Individualized GEC prediction*

Show prediction vs. data (GEC & GECkg) for

1. no adaptation in ageing and
2. defenestration
3. metabolic decrease.

Figure 5 *–GEC population variability*

Show GEC and GECkg in NHANES (experimental data & NHANES prediction) with the defenestration.